J. Mater. Environ. Sci. 7 (11) (2016) 4269-4289
ISSN : 2028-2508
CODEN: JMESCN

Corrosion Control of Carbon Steel in Hydrochloric Acid by New Eco-Friendly Picolinium-based ionic liquids Derivative: Electrochemical and Synergistic studies

A. Bousskri[1], A. Anejjar[1], R. Salghi[1,*], S. Jodeh[2], R. Touzani[3], L. Bazzi[4], H. Lgaz[1,5]
[1]*Laboratory of Applied Chemistry and Environment, ENSA, Université Ibn Zohr,PO Box 1136, 80000 Agadir, Morocco*
[2]*Department of Chemistry, An-Najah National University, P. O. Box 7, Nablus, Palestine.*
[3]*LCAE-URAC 18, Faculty of Science, University of Mohammed Premier, Po Box 717 60000 Oujda, Morocco.*
[4]*Department of chemistry,Team Applied Physical Chemistry, Laboratory Materials and Environment, University Ibn Zohr, Faculty of Science, Agadir, Morocco*
[5]*Laboratory separation processes, Faculty of Science, University Ibn Tofail PO Box 242, Kenitra, Morocco.*

Received 04 Jun 2016, Revised 29 Sept 2016, Accepted 6 Oct 2016
***Corresponding author. E-mail:** r.salghi@uiz.ac.ma*

Abstract

The corrosion behavior of C38 steel in HCl solution with different concentration of newly synthesized Picolinium-based Ionic liquids, *1-2-(4-Chloro Phenyl) 2-oxoethyl) -4N-Nmethyl) Picolinium bromide (CPOMPB)*, was investigated by weight loss and electrochemical measurements. Potentiodynamic polarization studies have shown that (*CPOMPB*) inhibition efficiency was found to increase with increase of the inhibitor concentrations to reach 87 % at 10^{-3}M of (*CPOMPB*), due to the adsorption of the inhibitor molecules on the metal surface and the adsorption follows Langmuir's adsorption isotherm. EIS spectra exhibit one capacitive loop and confirm the inhibitive ability. To elaborate the mechanism of corrosion inhibition, the kinetic and thermodynamic parameters for Carbon steel corrosion and inhibitor adsorption, respectively were determined and discussed. The effect of temperature on the corrosion behavior with the addition of (*CPOMPB*), was studied in the temperature range 298–328 K. Results obtained reveal that (*CPOMPB*) performs excellently as good corrosion inhibitor for C38 steel in 1.0 M HCl. X-ray photoelectron spectroscopic (XPS) analysis of the surface film was applied in order to get better understanding about the relationship between the inhibition efficiency and molecular structure and also to show the presence of the interfacial elements. The addition of potassium iodide (KI) enhanced the inhibition efficiency (E%). Most of the values of the synergism parameter (S_{θ}) calculated from inhibition efficiency was found to be greater than unity, suggesting that the phenomenon of synergism exists between *CPOMPB* and iodide ions. The adsorption of *CPOMPB* alone and in combination with *KI* followed Langmuir adsorption isotherm. The Optical microscopy (OM) was used for its morphological studies.

Keywords: *Corrosion, Steel, Inhibition, Picolinium-based Ionic liquids, Synergistic effect, Acid solution***.**

1. Introduction

Because of the general aggressively of acid solutions, inhibitors are commonly used to reduce the corrosive attack on metallic materials. The use of inhibitors is one of the most sensible methods for the protection of metals against corrosion in hydrochloric acid environment [1, 2]. There are various organic inhibitors which tend to decrease the corrosion rate of steel and iron in acidic solutions [3–7]. Over the years, tremendous efforts have been deployed aiming at finding suitable organic and inorganic corrosion inhibitors in various corrosive media [8-14]. Most effective are organic compounds containing electronegative functional groups and $\boldsymbol{\pi}$-electron in triple or conjugated double bonds as well as heteroatom like sulphur, phosphorus, nitrogen and oxygen are major actives adsorption centers [15-18]. The mode of adsorption depend on the chemical structure of the molecule, the chemical composition of the solution, the nature of the metal surface and the electrochemical potential of the metal-solution interface. The most important aspect of inhibition, normally considered by corrosion scientists is the relation between the molecular structure and corrosion inhibition efficiency [19-21]. Over the past two decades, Ionic liquids (ILs) have attracted considerable attention as friendly environmental substitutes for volatile organic solvents due to the several unique properties such as negligible vapor pressure, high thermal stability, easy recyclability, no flammability, and high ionic conductivity [22–25]. Generally, ILs are a group of low-melting-point salts containing organic cation, such as imidazolium, pyrrolidinium, or pyridazinium, paired with various anions, such as bromide or tetrafluoroborate [26].Due to these unique properties, ILs have been widely synthesized and investigated as media for electrodeposition of metals [27–29], catalysis and biocatalysis [30–35], corrosion inhibition [36–39], food chemical science [40], as a tool for lignocellulosic biomass fractionation [41], solvents in organic synthesis (42), electrolytes for electrochemical devices such as batteries [43, 44], in fuel cells [45], in polymer science [46], in dye-sensitized solar cells [47] and the nuclear industry [48]. On the other hand, numerous studies have demonstrated the antimicrobial activity of various classes of ionic liquids against both environmental and clinically important microorganisms [49–55]. According to the above mentioned, and our ongoing research, interest in ionic liquids inhibitive action we continued to examine the inhibitive action of a new synthesized Picolinium-based ionic liquids compound with green chemical processes under ultrasound and microwave irradiation, namely *1-2-(4-Chloro Phenyl) 2-oxoethyl) -4N-Nmethyl) Picolinium bromide (**CPOMPB**)*, on the behavior of carbon steel corrosion in 1M Hydrochloric acid solution. The effect of ILs concentration on the corrosion inhibition efficiency E(%) will be examined by weight loss measurements, polarization curves, impedance spectroscopy (EIS). The effect of temperature on E(%) will be investigated as well, leading to the understanding of the inhibition process kinetics and thermodynamics. The Optical microscopy (OM) was used for its morphological studies. In this study, the inhibitive effect of CPOMPB and its synergistic inhibition effect with iodide were also studied. The chemical structures of the studied Picolinium–based ionic liquids are given in Fig.1.

2. Experimental

2.1. Materials

The steel used in this study is a carbon steel (C38) (Euronorm: C35E carbon steel and US specification: SAE 1035). The chemical composition of carbon steel is given in Table1.

Table1: Chemical Composition of Carbon-Steel.

Elément	**Fe**	**C**	**Si**	**Mn**	**Cu**	**S**	**Cr**	**Co**	**Ti**	**Ni**
Wight %	Balance	0.37	0.23	0.68	0.16	0.016	0.077	0.09	0.011	0.059

2.2. Chemical Compound

Microwave-assisted synthesis and characterization of various imidazolium-based, piridinium-based, pyridazinium and picolinium-based ionic liquids (ILs) was reported in details by *Messali et al.* [56, 57, 58-60]. The structure of the investigated (ILs) in the current work, namely the *1-2-(4-Chloro Phenyl) 2-oxoethyl) -4N-Nmethyl) Picolinium bromide (**CPOMPB**)* is shown in Fig.1. In the following text, this compound will be denoted as (***CPOMPB***) for simplicity.

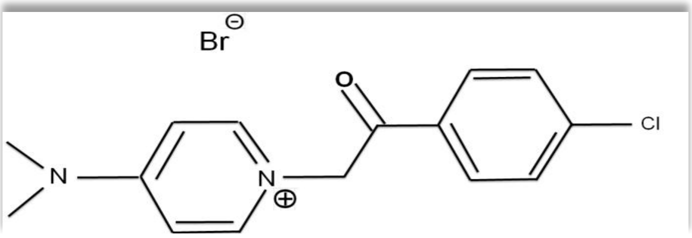

Figure 1: The chemical structure of 1-2-(4-Chloro Phenyl) 2-oxoethyl) -4N-Nmethyl) Picolinium bromide (**CPOMPB**).

2.3. Solutions

The aggressive solutions of 1.0 M Hcl were prepared by dilution of analytical grade 37% HCl with distilled water. The solution tests are freshly prepared before each experiment. The organic compound tested was the ionic liquid *1-2-(4-Chloro Phenyl) 2-oxoethyl) -4N-Nmethyl) Picolinium bromide* (***CPOMPB***). The concentration range of this compound was 10^{-3} to 10^{-6} M. Triplicate experiences were made to ensure the reproducibility.

2.4. Weight loss measurements

Coupons were cut into 2 × 2 × 0.08 cm^3 dimensions are used for weight loss measurements. Prior to all measurements, the exposed area was mechanically abraded with 180, 320, 800, 1200 grades of emery papers. The specimens were washed thoroughly with bidistilled water then with acetone to ensure the removal of all corrosion products, and finally degreased and dried with ethanol before weighing. Gravimetric measurements are carried out in a double walled glass cell equipped with a thermostated cooling condenser. The solution volume is 80 cm^3.

The immersion time for the weight loss is 6 h at 298 K. All experiments were duplicated to ensure reproducibility and the mean values are reported in the current work.

2.5. Electrochemical Tests

2.5.1. Electrochemical Impedance Spectroscopy (EIS)

The electrochemical measurements were carried out using Voltalab (Tacussel-Radiometer PGZ 100) potentiostat and controlled by Tacussel corrosion analysis software model (Voltamaster 4) under static condition. The corrosion cell used had three electrodes. The reference electrode was a saturated calomel electrode (SCE). A platinum electrode was used as auxiliary electrode. The working electrode was carbon steel. All potentials given in this study were referred to this reference electrode. The working electrode was immersed in test solution for 30 minutes to establish a steady state open circuit potential (Eocp). After measuring the Eocp, the electrochemical measurements were performed. All electrochemical tests have been performed in aerated solutions at 298 K. The EIS experiments were conducted in the frequency range with high limit of 100 kHz and different low limit 0.1 Hz at open circuit potential, with 10 points per decade, at the rest potential, after 30 min of acid immersion, by applying 10 mV ac voltage peak-to-peak. Nyquist plots were made from these experiments. The best semicircle can be fit through the data points in the Nyquist plot using a non-linear least square fit so as to give the intersections with the **x**-axis.

2.5.2. Potentiodynamic polarization

The electrochemical behaviour of carbon steel sample in inhibited and uninhibited solution was studied by recording anodic and cathodic potentiodynamic polarization curves. Measurements were performed in the 1.0 M HCl solution containing different concentrations of the tested inhibitor by changing the electrode potential automatically from -800 mV to -200 mV versus corrosion potential at a scan rate of 1 $mV.s^{-1}$. The linear Tafel segments of anodic and cathodic curves were extrapolated to corrosion potential to obtain corrosion current densities (I_{corr}).

2.6. Optical microscopies (OM)

Immersion corrosion analysis of carbon steel samples in the acidic solutions with and without the optimal concentration of the inhibitor was performed using OM. Immediately after the corrosion tests, the samples were subjected to OM studies to know the surface morphology. OM ***BestScope*** was used for the experiments.

3. *Results and Discussion*

3.1. Electrochemical Impedance Spectroscopy Measurements (EIS)

3.1.1. Concentration effect

The corrosion behavior of carbon steel in 1 M HCl solution in the presence of *CPOMPB* was investigated by (EIS) at room temperature after 30 min of immersion. The Nyquist plots for carbon steel obtained at the interface in the presence and absence of *CPOMPB* at different concentrations are given in Fig 2.

The charge-transfer resistance (R_{ct}) values are calculated from the difference in impedance at lower and higher frequencies, as suggested by Tsuru et al [61]. The double layer capacitance (C_{dl}) and the frequency at which the imaginary component of the impedance is maximal ($-Z_{max}$) are found as represented in equation 1:

$$C_{dl} = \frac{1}{\omega \ R_{ct}} \quad \text{where} \quad \omega = 2\pi f_{max} \qquad (1)$$

As observed, the Nyquist plots contain a depressed semi-circle with the center below the real X-axis, which is size increased by increasing the inhibitor concentrations, indicating that the corrosion is mainly a charge transfer process [62] and the formed inhibitive film was strengthened by the addition of the inhibitor *CPOMPB*. The impedance parameters derived from these plots are shown in Table3.

The equivalent circuit:

The quantitative analysis of the electrochemical impedance spectra (EIS) was studied based on a physical model of the corrosion process with hydrogen depolarization and with charge transfer controlling step. The simplest model includes the charge transfer resistance (**R_t**) in parallel to the capacitance (**C_{dl}**) connected with the electrolyte resistance (**R_e**). The equivalent circuit model employed for this system is presented in Fig.3.

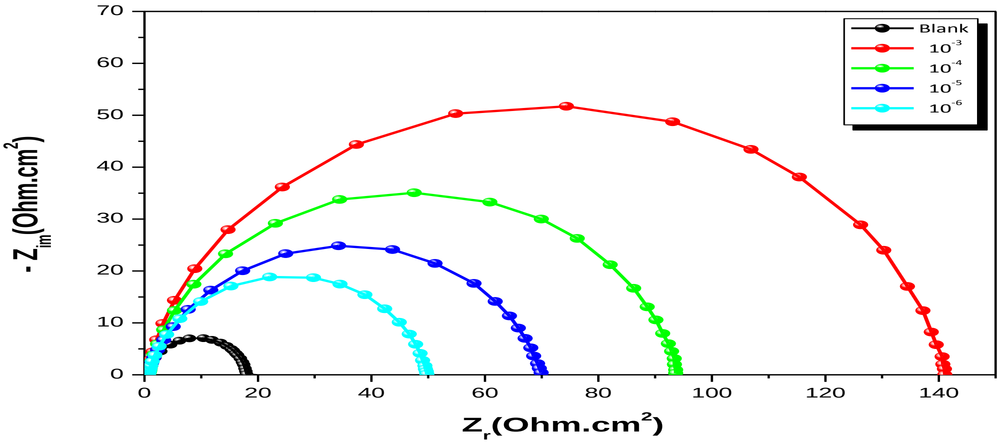

Figure 2: Nyquist plots for carbon steel in 1 M HCl containing different concentrations of *CPOMPB*.

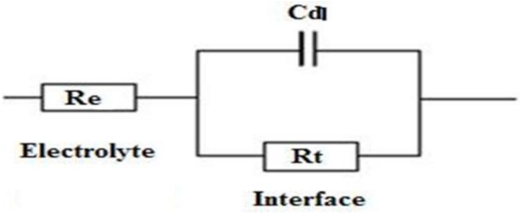

Figure 3: The standard Randle circuit.

This percent inhibition efficiency is calculated by charge transfer resistance obtained from Nyquist plots, according to the equation2:

$$E_{Rct} \ \% = \frac{R'_{ct} - R_{ct}}{R'_{ct}} \times 100 \qquad (2)$$

Where R_{ct} and R'_{ct} are the charge transfer resistance values without and with inhibitor, respectively.

From the Table .2 we can see in the presence of the *CPOMPB* the values of R_{ct} has enhanced and the values of double layer capacitance C_{dl} are also brought down to the maximum extent with the increasing of the inhibitors concentration. The decrease in C_{dl} shows that the adsorption of the inhibitors takes place on the metal surface in acidic solution; which can result from a decrease in local dielectric constant and/or an increase in the thickness of the electric double layer [63].

Table 2: Electrochemical Impedance for corrosion of steel in acid medium at various concentrations of *CPOMPB.*

Inhibitor	***Conc (M)***	***Rct (Ω.cm²)***	***C_{dl} (µF/cm²)***	***E_{Rct} (%)***
Blank	1	18	177	-
CPOMPB	**1×10^{-3}**	141	45.17	**87**
	1×10^{-4}	94	48.40	81
	1×10^{-5}	69	57.69	74
	1×10^{-6}	49	81.24	63

From Table.2 we can also see that the inhibition efficiency increases with the increasing inhibitor concentration and the maximum percentage of inhibition efficiency (E_{Rct} %) was achieved at the concentration of 10^{-3}M (**87**%). The results obtained by this method are in good agreement with the values of inhibitor efficiency obtained from polarization measurements.

3.1.2. KI influence (Synergetic effect)

It is also observed that the shapes of the impedance plots for the inhibited electrodes with the presence of KI are different from those of the uninhibited electrodes and reveals that the presence of *CPOMPB* in 1M HCl solutions increases the charge transfer impedance due to the formation of protection layer on the steel surface, but it does not change other aspects of the corrosion behavior. For these impedance spectra, it is essential to develop the appropriate physical models which can be used to fit the experimental data and then extract the parameters which characterize the corrosion process. Fig.5 shows the equivalent circuit model used to fit the experimental impedance data of carbon steel in 1M HCl containing *CPOMPB+KI*. In this case R*s* refers to the solution resistance, CPE the constant phase element, R1 the polarization resistance, and R1 + R2 present the charge transfer resistance (R_{ct}). Resistance R2 and CPE2 may be correlated with a slow low frequency intermediate process [64]. It should be noticed that the depressed capacitive loops at the higher frequencies appear in Fig. 4.

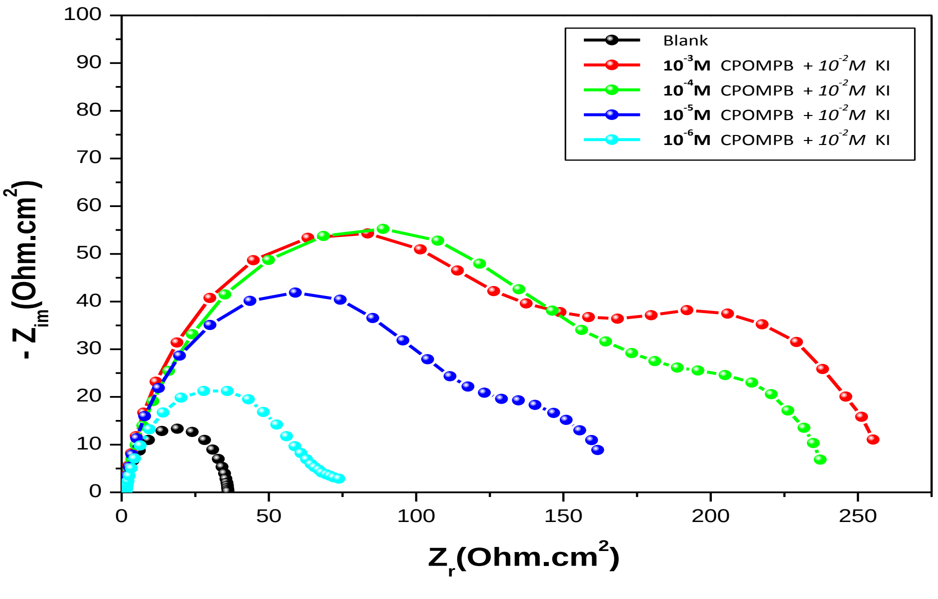

Figure 4: Nyquist plots (synergistic effect) for Carbon steel specimens in 1M HCl solution.

Deviation of this kind, often referred to as frequency dispersion, was attributed to roughness and inhomogeneities of the solid surface [65]. Therefore, a constant phase element (CPE) instead of a capacitive element is used in Fig.5 to get a more accurate fit of experimental data sets. The impedance of the CPE is expressed as:

$$Z_{\mathrm{CPE}} = A^{-1}(j\omega)^{-n}$$

where A is the magnitude of CPE (in $\Omega^{-1}S^{n}\ cm^{-2}$), ω is the sine wave modulation angular frequency (in rad S^{-1}), $j^2 = -1$ is the imaginary number, and n is an empirical exponent ($0 \leq n \leq 1$) which measures the deviation from the ideal capacitive behavior [66].

Fig. 4 represents the Nyquist plots of carbon steel in 1M HCl in the presence of various concentrations of inhibitor + KI.

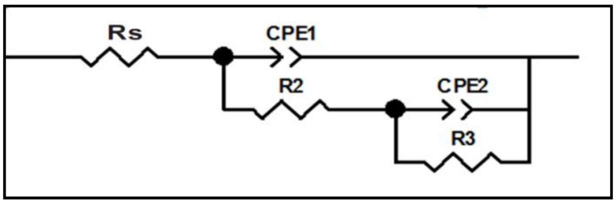

Figure 5: Electrical equivalent circuit model used to fit the EIS data of the interface Carbon steel/1.0 M HCl solution with *CPOMPB* inhibitor.

Fig.6 reports an example (Nyquist formats) of the relative fit obtained with the circuit model of Fig.5.

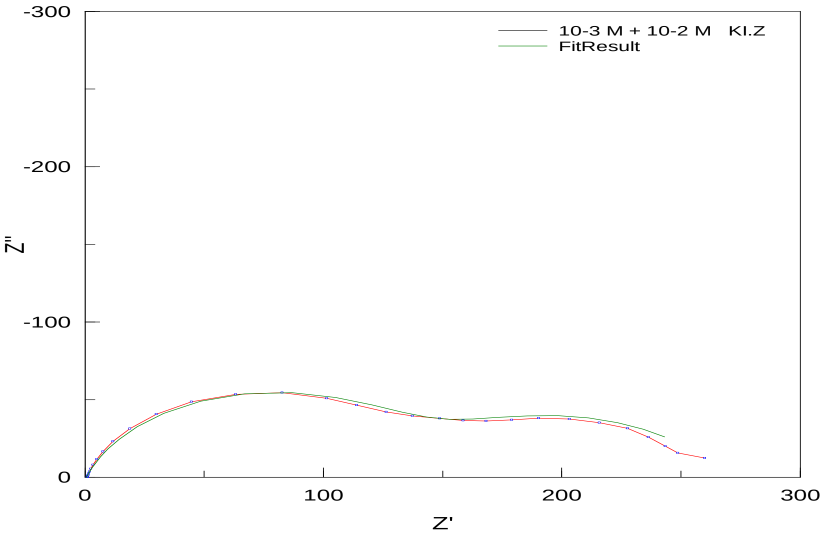

Figure 6: EIS Nyquist diagrams for carbon steel in 1M HCl /10^{-2}M KI +10^{-3}M *CPOMPB* interface: (—) experimental; (—) fitted data using circuit in *Fig.5*.

It is clear that the proposed model is well representative of the phenomena which may occur in the investigated system, both in the HF and in the LF parts of the spectra. The impedance parameters and fitting results derived from these studies using *Z-view* software are summarized in *Table 5*. In this table are shown also the calculated double layer capacitance (C_{dl}) derived from the CPE parameters according to the equation [67]:

$$C_{\mathrm{dl}} = \left(AR_{ct}{}^{1-n}\right)^{1/n}$$

Table 3: Impedance parameters and inhibition Efficiency values for carbon steel in 1M HCl solution containing different concentrations of *CPOMPB* + 10^{-2} M of KI at 298 K.

Conc. (M)	Rs ($\Omega.cm^2$)	CPE1 ($S^n/\Omega.cm^2$)	*n*1	R2 ($\Omega.cm^2$)	C_{dl} µF/cm2	CPE2 ($S^n/\Omega.cm^2$)	*n*2	R3 ($\Omega.cm^2$)	R_{CT} ($\Omega.cm^2$)	E_{Rct} %
Blank	0.59	0.000122	0.87	18	48.96	0.00188	0.56	0.2	18.2	-
10^{-3} M CPOMPB + 10^{-2} KI	0.59	0.0002	0.79	148	91.88	0.0095	0.65	120	268	93.2
10^{-4} M CPOMPB + 10^{-2} KI	0.59	0.00022	0.78	144	96.42	0.010556	0.55	100	244	92.5
10^{-5} M CPOMPB + 10^{-2} KI	0.59	0.00019	0.86	100	108.66	0.0095	0.52	70	170	89.2
10^{-6} M CPOMPB + 10^{-2} KI	0.59	0.00035	0.78	60	118.81	0.007	0.55	2	62	70.6

Inspection of data in the Table 3 clearly shows that the impedance response of metal specimens has marked difference in the absence and presence of the KI with inhibitor *CPOMPB*. it is clear that R_{ct} values are increased with increasing inhibitor concentration. The capacitance values C_{dl} decreases with inhibitor concentration and this decrease in C_{dl} is enhanced upon addition of I^- ions to the corrosive environment. These results suggest that the *CPOMPB* molecules function by adsorption at the metal/solution interface [68] and this adsorption is reinforced by I^- ions. This decrease in C_{dl} may be explained on the basis that the double layer between the charged metal surface and the solution is considered as an electrical capacitor. The E_{Rct} % data reveal that the corrosion inhibition capacity of *CPOMPB* is markedly enhanced by the addition of KI.

The Nyquist plot of carbon steel in 1 M HCl containing 10^{-3} M of *CPOMPB* in combination with 10^{-2} M of KI is shown in Fig.7. The results show that the diameters of the semicircles in Nyquist plot increases with addition of KI. The impedance data were analyzed using the equivalent circuit shown in Fig.5 and the corresponding electrochemical parameters are given in Table 3. The inhibition efficiency increased from 87% in the presence of *CPOMPB* to 93.21% on addition of KI to *CPOMPB* solution, the enhanced inhibition efficiency noted for *CPOMPB* on addition of I^- ions is due to synergistic effect.

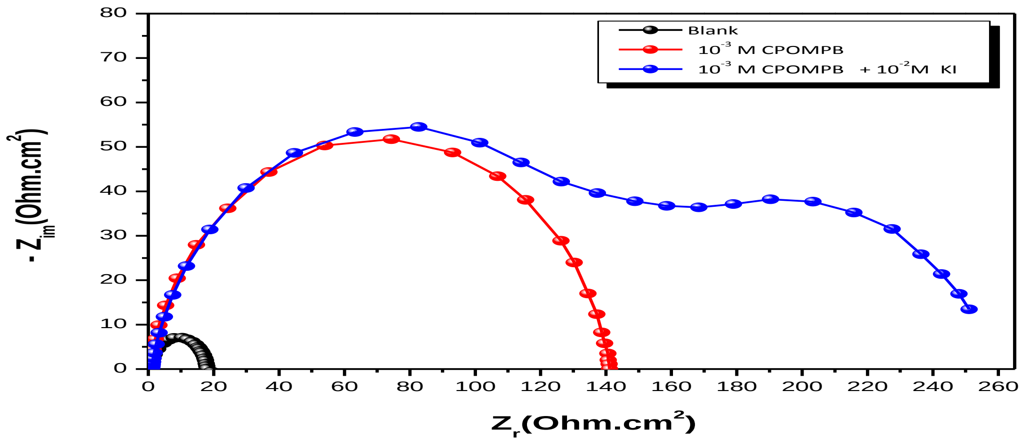

Figure 7: Nyquist plots for carbon steel recorded in 1 M HCl + 10^{-3}M *CPOMPB* solution in the absence and presence of KI at 298 K.

3.2. Potentiodynamic Polarization Curves

3.2.1. Concentration effect

The effect of *CPOMPB* on the corrosion reactions was determined by polarization techniques. The changes observed in the polarization curves after the addition of the inhibitor are usually used as the criteria to classify inhibitors as cathodic, anodic or mixed [69-70].

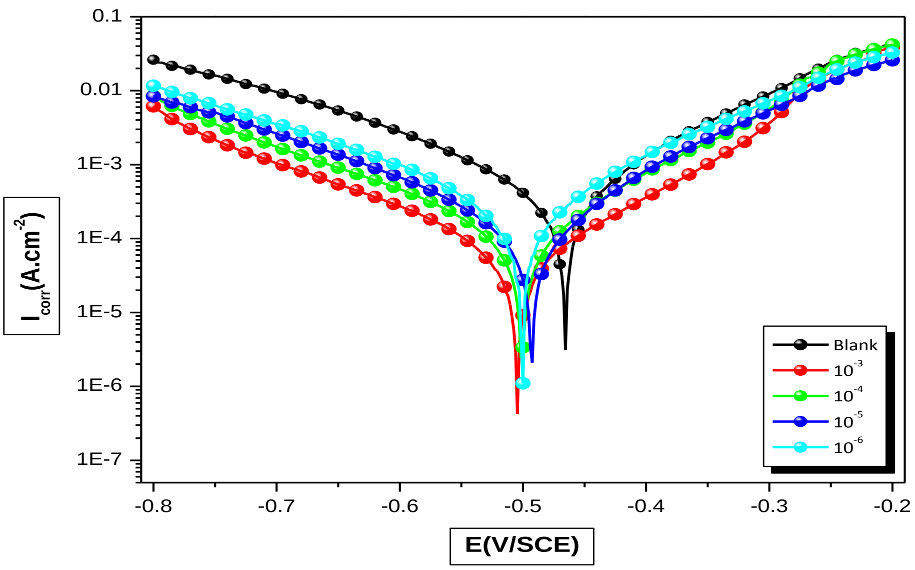

Figure 8: Potentiodynamic polarization curves of C38 steel in 1M HCl in the presence of different concentrations of *CPOMPB* at 298 K.

Fig.8 shows the Tafel polarization curves for carbon steel in 1.0 M chloridric acid solution at different concentrations (10^{-3} to 10^{-6} M) of inhibitor at 298 K. The potentiodynamic parameters (Table 4) such as corrosion potential (E_{corr}), cathodic Tafel slopes (b_c), corrosion current density (I_{corr}), were obtained from Tafel plots and the inhibition efficiency values E_I(%), were calculated using equation3.

$$E_I \ \% = \frac{I_{corr} - I'_{corr}}{I_{corr}} \times 100 \qquad (3)$$

Where I_{corr} and I'_{corr} are uninhibited and inhibited corrosion current densities, respectively.

The results from Fig.4 and Table 4 indicate that the corrosion potential is more negative and the corrosion current density (I_{corr}) decreases in the presence of the inhibitor compared to the blank solution and also with increasing the inhibitor concentration which suggest that the presence of this compound retards the dissolution of carbon steel electrodes in a 1M HCl solution. This result confirms the inhibitive action of the *CPOMPB* toward acid corrosion of steel [71]. This implies that *CPOMPB* affected both the anodic dissolution of carbon steel electrodes and it's cathodic reduction in hydrogen evolution reactions, indicating that the *CPOMPB* compound could be classified as a mixed-type inhibitor. This due to the adsorption of the inhibitor over the corroding surface [72, 73]. These polarization curves tests were in good agreement with the corrosion weight loss and impedance measurements.

Table 4: Electrochemical parameters of carbon steel in 1M HCl solution without and with *CPOMPB* at different concentrations.

Inhibitor	***Conc (M)***	***-E_{corr} (mV/SCE)***	***I_{corr} (µA/cm^2)***	***-b_c (mV/dec)***	***E_I (%)***
Blank	1.0	469	588	168	-
CPOMPB	1×10^{-3}	507	70	178	**88.10**
	1×10^{-4}	503	115	143	80.44
	1×10^{-5}	496	155	170	73.64
	1×10^{-6}	503	230	171	60.88

The inspection of results in Table3 indicate that *CPOMPB* inhibits the corrosion process in the studied range of concentrations and E_I (%) increases with C_{inh}, reaching its maximum value, **88.10**%, at 10^{-3}M, due to the increase in the blocked fraction of the electrode surface by adsorption.The values of the cathodic Tafel lines b*c*, show slight changes with the addition of *CPOMPB*.This result means that the mechanism at the electrode reactions is not changed [74].

3.2.2. KI influence (Synergistic effect)

Potentiodynamic polarization curves for *CPOMPB* in 1M Hcl solution at 298 K for Carbon steel in the presence of various concentrations of inhibitor + KI are shown in *Fig 9*. Polarization parameters are listed in *Table 5*. The data show that, addition of the inhibitor to acid media affected both the cathodic and anodic parts of the curves. Addition of I− ions to *CPOMPB*/HCl systems results in marked decrease in the corrosion current density (I_{corr}). From the values it is clear that the inhibition efficiency of *CPOMPB* alone is increased in presence of KI. These results also confirm the existence of strong synergism between *CPOMPB* and KI in the corrosion inhibition of Carbon steel in these solutions. Furthermore, we see from Table 5, firstly an increase in inhibitory activity compared with that of *CPOMPB* alone and , on the other hand, a shift in the corrosion potential towards the positive values under the effect of the presence of KI . This result can be explained by the adsorption of I^- ions to the steel surface which results in favor of that of the low *CPOMPB* potential. The inhibition efficiency increased from 88.10 % in the presence of *CPOMPB* to 94.39 % on addition of KI to *CPOMPB* solution.

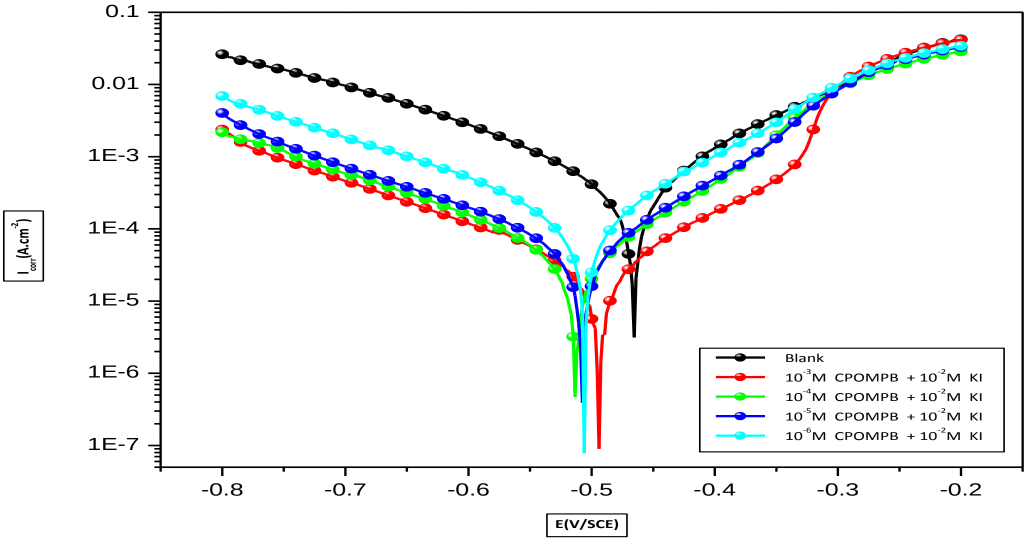

Figure 9: Potentiodynamic polarization curves of C38 steel in 1M HCl in the presence of different concentrations of *CPOMPB* + 10^{-2} M KI at 298 K.

Table 5: Polarization parameters of C38 steel in 1M HCl at 298 K in the absence and presence of *CPOMPB* + 10^{-2}M KI.

C (M)	-Ecorr (mV/SCE)	Icorr (µA/cm²)	-βc (mV/dec)	E (%)
Blank	469	588	168	-
10^{-3} M CPOMPB + 10^{-2} KI	496	33	194	**94.39**
10^{-4} M CPOMPB + 10^{-2} KI	515	51	143	91.33
10^{-5} M CPOMPB + 10^{-2} KI	510	59	170	89.97
10^{-6} M CPOMPB + 10^{-2} KI	508	158	171	73.13

3.3. *Weight Loss Measurements and Adsorption Isotherm*

Weight loss measurement was done according to the method described previously [75]. And is a non-electrochemical technique for the determination of corrosion rates and inhibitor efficiency which provides more reliable results than electrochemical techniques because the experimental conditions are approached in a more realistic manner yet the immersions tests are time-consuming [76-77]. Therefore, due to such differences (experimental conditions), the values would obviously differ from the electrochemical values.

The action of an inhibitor in aggressive acid media is assumed to be due to its adsorption at the metal/solution interface. The adsorption process depends on the electronic characteristics of the inhibitor, the nature of metal surface, temperature, steric effects and the varying degrees of surface-site activity [78, 79].

All the tests were conducted in aerated 1.0M HCl at 298 K with different concentrations of *CPOMPB.* And the Values of the inhibition efficiency and corrosion rate obtained from the weight loss measurements of C-steel for different concentrations of *CPOMPB* in 1.0M HCl at 298 K after 6h of immersion are given in Table 6. After the elapsed time, the specimen were taken out, washed, dried and weighed accurately.

The inhibition efficiency (E_w%) and surface coverage (θ) were determined by using the following equations:

$$E_w\ \% = \frac{W_{corr} - W'_{corr}}{W_{corr}} \times 100 \qquad (5)$$

$$\theta = 1 - \frac{W'corr}{Wcorr} \qquad \text{Where} \qquad \theta = \frac{E_W\,(\%)}{100} \qquad (6)$$

Where W_{corr} and W'_{corr} are the corrosion rates of Carbon steel due to the dissolution in 1.0M HCl in the absence and the presence of definite concentration of inhibitor, respectively, and ***θ*** is the degree of surface coverage of the inhibitor.

Table 6: Weight loss data of mild steel in 1 M HCl for various concentration of the *CPOMPB.*

Inhibitor	***Conc (M)***	***W_{corr} (mg. cm^{-2} h^{-1})***	***E_w (%)***	***θ***
Blank	0	1,001	-	-
CPOMPB	1×10^{-3}	0.129	**87.11**	0.871
	1×10^{-4}	0.185	81.52	0.815
	1×10^{-5}	0.265	73.53	0.735
	1×10^{-6}	0.365	63.54	0.635

It can be seen from Table 4, that inhibitor *CPOMPB* inhibits the corrosion of C-steel and efficiency increases with the increasing inhibitors concentration.

The variations in the degree of surface coverage and inhibition efficiency with *CPOMPB* concentration shown in Fig.10 suggest that *CPOMPB* inhibits steel at all the concentration range used in the study. Maximum degree of surface coverage ***θ*** was reported at 10^{-3}M concentration of this compound.

Adsorption Isotherm:

In order to understand the mechanism of corrosion inhibition, the adsorption behavior of the adsorbate on the carbon steel surface must be known. Two main types of interaction can describe the adsorption of the molecule of *CPOMPB,* physisorption and chemisorption. These are influenced by the chemical structure of the inhibitor, the type of the electrolyte and the charge and nature of the metal.

The information on the interaction between the inhibitor molecule of *CPOMPB* and the metal surface can be provided by adsorption isotherm. The degree of surface coverage (***θ***) for different concentrations of inhibitor was evaluated from Weight loss measurements. Attempts were made to fit ***θ*** values to various isotherms including Frumkin, Temkin and Langmiur.

It was found that the data best fit was obtained with the Langmiur isotherm Fig 3. According to this isotherm θ is related to concentration inhibitor [80].

$$\frac{\theta}{1-\theta} = K_{ads}.C_{inh} \qquad (7)$$

By rearranging this equation:

$$\frac{C_{inh}}{\theta} = \frac{1}{K_{ads}} + C_{inh} \qquad (8)$$

Where K_{ads} is the adsorption/desorption equilibrium constant, C_{inh} is the corrosion inhibitor concentration in the solution

$$\log K = -1{,}74 - \left(- \frac{\Delta G^{0}_{ads}}{2{,}303RT} \right) \qquad (9)$$

Where ΔG^{0}_{ads} is the free energy of adsorption.

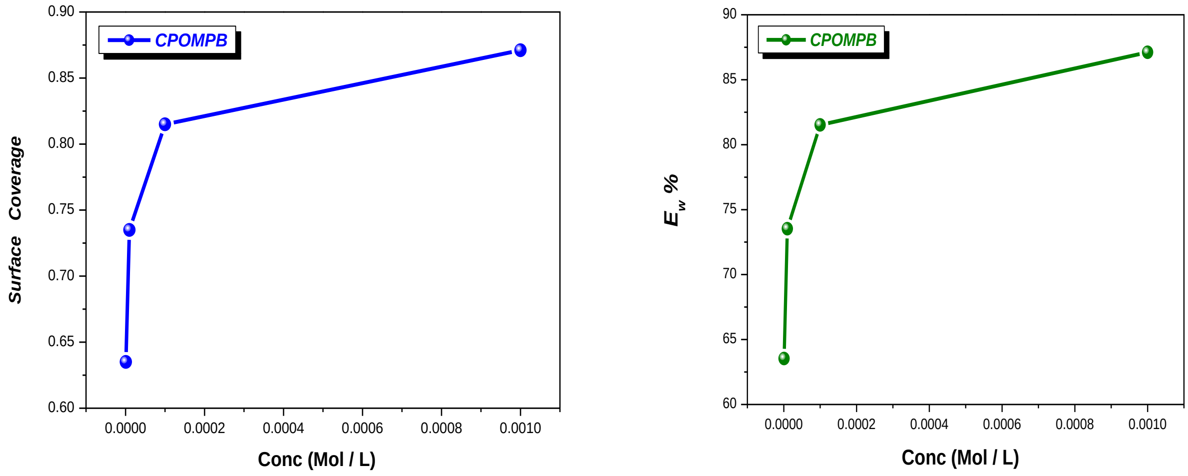

Figure 10: Variation of inhibition efficiency and surface coverage in 1M HCl on C-steel surface without and with different concentrations of *CPOMPB.*

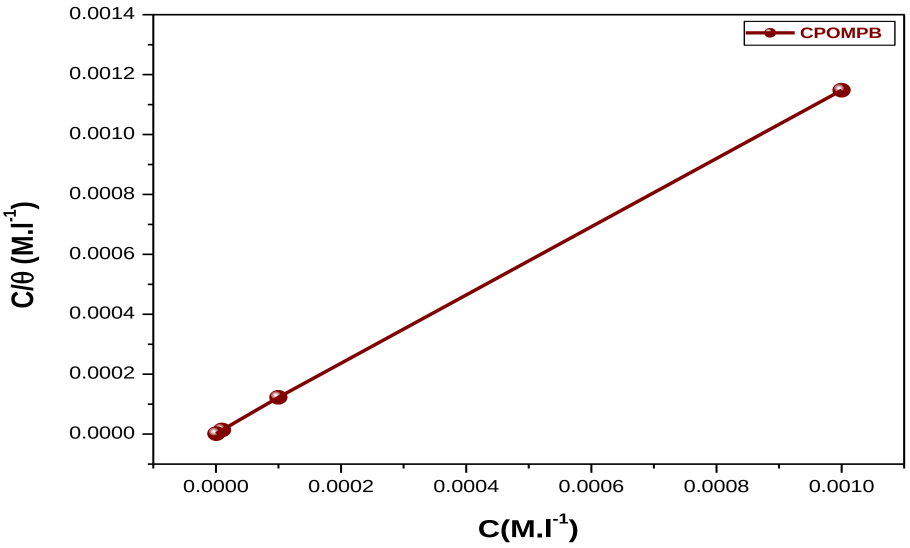

Figure 11: Plots of Langmuir adsorption isotherm of *CPOMPB* on the steel surface at 298K.

It was found that Fig 11. (Plot of $\frac{C}{\theta}$ versus C) gives straight line with slope near to 1, indicating that the adsorption of compound under consideration on Carbon steel / acidic solution interface obeys Langmiur's adsorption.

Table 7: The thermodynamic parameters for the corrosion of carbon steel in 1 M HCl in the absence and presence of different concentrations of *CPOMPB*.

Inhibitor	***Slope***	***K_{ads} (M^{-1})***	***R^2***	***ΔG^0_{ads} (kJ/mol)***
CPOMPB	1.14496	291000	0.99998	**-41.10**

The free energy of adsorption ΔG^0_{ads} can be calculated from the K_{ads} value obtained from the above correlation:

$$\Delta G_{ads} = -RT\ \ln(55.5\ \text{x}\ K_{ads}) \qquad (10)$$

where 55.5 is the concentration of water, R is the universal gas constant and T is the absolute temperature.

The adsorption–desorption equilibrium constant K_{ads}, was determined as 10^{-3} M, leading to ΔG^0_{ads} = **-41.10** kJ.mol^{-1} for *CPOMPB* at the temperature of 298 K. The large K_{ads} value gives better inhibition efficiency due to strong electrical interaction between the double layer and adsorbing inhibitor molecules while a small K_{ads} value compromise that such interactions between the adsorbing inhibitor molecules and the metal surface are weaker, indicating that the inhibitor molecules are easily removable by the solvent molecule from the surface [81]. The negative sign of ΔG^0_{ads} indicates the spontaneity of the adsorption process and stability of the adsorbed layer on the electrode surface [82]. Generally, the values of ΔG^0_{ads} around -20 kJ mol^{-1} or less negative are known to be associated with physical adsorption (electrostatic interactions between the inhibitor and charged surface) while those around - 40 kJ .mol^{-1} or more negative are known to be associated with chemisorption (charge sharing or transferring from organic molecules to the metal surface and form a coordinate type of metal bond) [83]. From this estimation, it can be concluded that the *CPOMPB* is chemically adsorbed on the charged C-steel surface. Results obtained from gravimetric measurements show that the steel corrosion rate values decrease when the concentration of *CPOMPB* increases (Fig.12). The corrosion inhibition can be attributed to the adsorption of the inhibitor at the steel/acid solution interface. This result suggests that increase in inhibitor concentration increases the number of molecules adsorbed onto steel surface and reduces the surface area that is available for the direct acid attack on the metal surface. The highest inhibition efficiency 87.11 % was obtained at 10^{-3}M of *CPOMPB*. The inhibition efficiencies, calculated from weight loss measurements, show the same trend as those obtained from electrochemical studies (Fig.12).

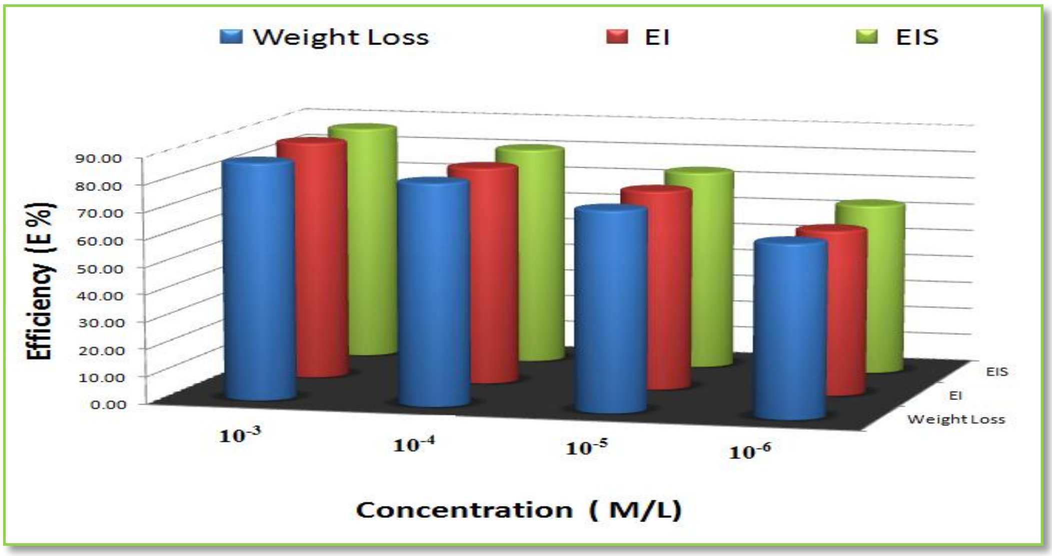

Figure 12: Comparison of inhibition efficiency (E %) values obtained by weight loss, EI and EIS methods.

KI influence:

Weight loss of carbon steel in 1M HCl solution at 298 K was determined at various concentrations of *CPOMPB* + 10^{-2} M KI. The corrosion rates, inhibition efficiencies, and surface coverage (Θ) in the presence of inhibitor + KI are shown in the Table 7. It is also clear that the corrosion rate markedly decreased with inhibitor concentration. This response is due to the fact that the surface coverage (Θ) of the inhibitor molecules on the metal through adsorption increases with increase in concentration. The inhibitor + KI system showed similar trend.

From Table7 it is evident that the inhibition efficiency increased with increase in concentration. At the inhibitor concentration of 10^{-3}M, the maximum E_w% was 87.21%, whereas in the presence of constant KI concentration we see the evolution of the inhibition efficiency E_w% reaching 94.11%, so it was found that the combination of inhibitor and KI has better inhibition efficiency for all studied inhibitor concentrations.

Table 8: Calculated values of inhibition efficiency (***Ew*** %) of carbon steel in 1 M HCl for different concentration of *CPOMPB* with and without KI.

Inhibitor/Conc (M/L)	W_{corr} (mg. cm^{-2})	Ew (%)	θ
Blank	1.001	-	
Blank + 10^{-2} M KI	0.501	49.950	0.500
10^{-3} M CPOMPB	0.128	**87.213**	0.872
10^{-4} M CPOMPB	0.185	81.518	0.815
10^{-5} M CPOMPB	0.265	73.526	0.735
10^{-6} M CPOMPB	0.365	63.536	0.635
10^{-3} M CPOMPB + 10^{-2} M KI	0.059	**94.109**	0.941
10^{-4} M CPOMPB + 10^{-2} M KI	0.082	91.798	0.918
10^{-5} M CPOMPB + 10^{-2} M KI	0.097	90.290	0.903
10^{-6} M CPOMPB + 10^{-2} M KI	0.236	76.424	0.764

Adsorption Isotherm and Free Energy of Adsorption:

Fig 13. represent the adsorption plot of *CPOMPB* + KI obtained by the weight loss measurements of carbon steel in 1M HCl solution at 298 K. In the present investigation, *CPOMPB* + KI molecules showed ΔG^0ads= −43.91 for carbon steel in 1 M HCl suggesting that the adsorption of inhibitor is adsorbed strongly on the metal surface through coordinate type bond (chemisorption) [84,85], Table 9.

Parameter of synergism S_Θ:

The addition of KI drastically increases the E_w% values; From Table 10 it is clear that E_w% for KI in combination with inhibitor is higher than E_w% for single inhibitor, it is the synergistic effect. Aramaki and Hackerman [86] calculated the synergism parameter using the following equation:

$$S_\Theta = \frac{1-\Theta_{1+2}}{1-\Theta'_{1+2}}$$

Where $\Theta_{1+2} = (\Theta_1 + \Theta_2) - (\Theta_1 \Theta_2)$, Θ1 = surface coverage by anion; Θ_2 = surface coverage by cation, Θ'_{1+2} = measured surface coverage by both anion and cation. S_Θ approaches unity when there are no interactions between the inhibitor compounds, while $S_\Theta > 1$ points to a synergistic effect; in the case of $S_\Theta < 1$, the antagonistic interaction prevails. The values of the synergism parameter for the various concentrations of *CPOMPB* studied from the gravimetric analysis are presented in Table 10. Most of the values shown in this table are greater than unity. This is an indication that the enhanced inhibition efficiency resulting from the addition of iodide ions to *CPOMPB* is synergistic in nature [87].

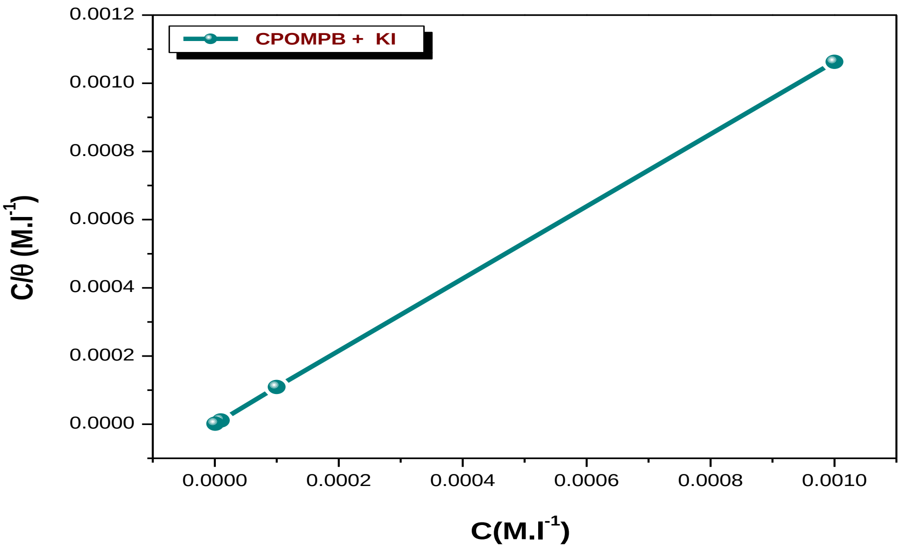

Figure 13: Langmuir adsorption isotherm for adsorption of *CPOMPB* + 10^{-2}M of KI on the C38 steel surface in 1M Hcl solution

Table 9: Thermodynamic parameters for the adsorption of *CPOMPB* + 10^{-2} M of KI in 1M Hcl on the carbon steel at 298K.

Inhibitor	**Slope**	**K_{ads} (M^{-1})**	**R^2**	**ΔG^0_{ads} (kJ/mol)**
CPOMPB + KI	1.0617	906000	0.9999	**-43.91**

The synergistic inhibition brought about by the combination of *CPOMPB* and iodide ions for the corrosion of carbon steel in 1M HCl solution can be explained on the basis that halide ions have a greater tendency to be adsorbed on the surface in attraction with organic cations. The protonated molecule of the inhibitor (*CPOMPB* $^+$) is then adsorbed by electrostatic attraction at the steel surface, where iodide ions are already adsorbed by chemisorption.

Table 10: Synergism parameter (S_θ) for different concentrations of *CPOMPB* in combination with 10^{-2} M of KI.

Concentration (M)	**Synergism parameter S_Θ**
10^{-3} M	1.09
10^{-4} M	1.13
10^{-5} M	1.37
10^{-6} M	0.77

3.4. *Effect of temperature*

3.4.1. Kinetics and thermodynamics:

The study on the effect of temperature on the corrosion rate and inhibition efficiency facilitates the calculation of kinetic and thermodynamic parameters for the inhibition and the adsorption processes. These parameters are useful in interpreting the type of adsorption by the inhibitor.

To investigate the mechanism of inhibition and to calculate the activation energies of the corrosion process, EIS measurement were taken at various temperatures in the absence and the presence of 10^{-3}M of *CPOMPB* (Fig 14 and 15)

The results reported in Table 11 showed the R_{ct} (resistance transfer) values decreases with increasing temperature in the absence and the presence of *CPOMPB.*

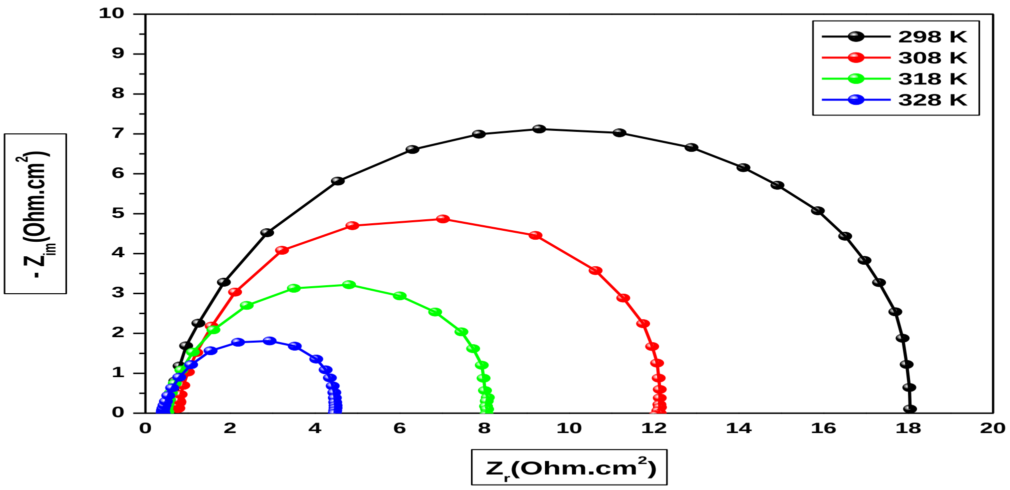

Figure 14: Nyquist diagrams for C38 steel in 1.0 M HCl at different temperatures.

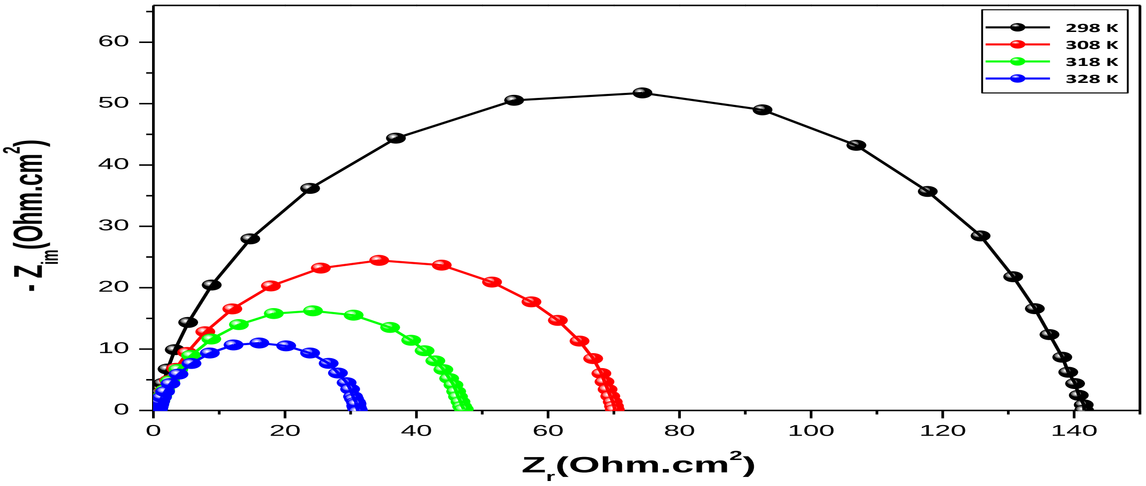

Figure 15: Nyquist diagrams for C38 steel in 1 M HCl + 10^{-3} M of *CPOMPB* at different temperatures.

Table 11: Thermodynamic parameters for the adsorption of *CPOMPB* in 1.0 M HCl on the C38 steel at different temperatures.

Inhibitor	Temp (K)	R_{ct} (Ω.cm^2)	C_{dl} (μF/cm^2)	E_{Rct} (%)
Blank	298	18	177	-
	308	12	190	-
	318	8	199	-
	328	4,5	223	-
NPOMPB	298	141	45	87.23
	308	70	57	82.86
	318	47	58	82.98
	328	31	64	85.48

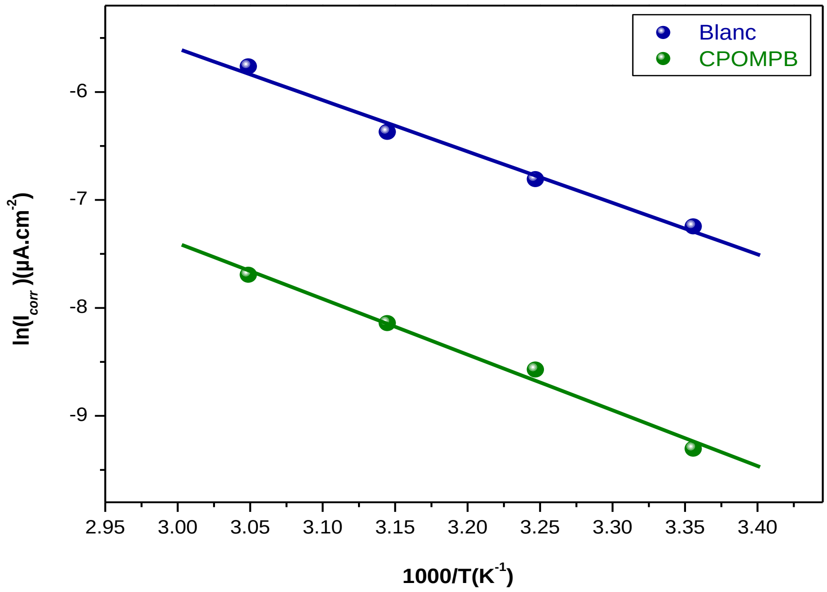

Figure 16: Arrhenius plots of C38 steel in 1 M HCl with and without 10^{-3}M of *CPOMPB*.

Also inhibition efficiency of *CPOMPB* remains without substantial change with increase in temperature.
Values of R_{ct} were employed to calculate values of the corrosion current density (I_{corr}) at various temperatures in absence and presence of *CPOMPB* using the following equation [88]:

$$I_{corr} = R_{ct}.T(z.F.R_{ct})^{-1} \tag{9}$$

Where R is the universal gas constant (R = 8.31 J K-1mol^{-1}), T is the absolute temperature, z is the valence of iron (z = 2), F is the Faraday constant (F = 96.485 coulomb) and R_{ct} is the charge transfer resistance.

Fig. 16 also shows that the corrosion reaction can be regarded as an Arrhenius-type process (Eq 9). The activation parameters for the studied system (E_a, ΔH_a^* and ΔS_a^*) were estimated from the Arrhenius equation and transition state equation (Eq 10-11):

$$I_{corr} = A\exp\left(\frac{-E_a}{RT}\right) \quad \text{Where} \quad \log I = -\frac{E_a}{2.303\,RT} + \log A \tag{10}$$

$$I_{corr} = \frac{RT}{Nh}\exp\left(\frac{\Delta S_a^*}{R}\right)\exp\left(-\frac{\Delta H_a^*}{RT}\right) \tag{11}$$

Where A is Arrhenius factor, E_a is the apparent activation corrosion energy, N is the Avogadro's number, h is the Plank's constant, and ΔH_a^* and ΔS_a^* are the enthalpy and the entropy changes of activation corrosion energies for the transition state complex. R is the perfect gas constant. The apparent activation energy was determined from the slopes of Ln I_{corr} vs 1/T graph depicted in Fig.16.

A plot of ln (I_{corr}/T) against 1/T (Fig. 17) gave a straight line with slope (ΔH_a^* /R) and intercept (ln(R/N A h) + (ΔS_a^* /R)), from which the values of ΔH_a^* and ΔS_a^* were calculated and listed in Table 12.

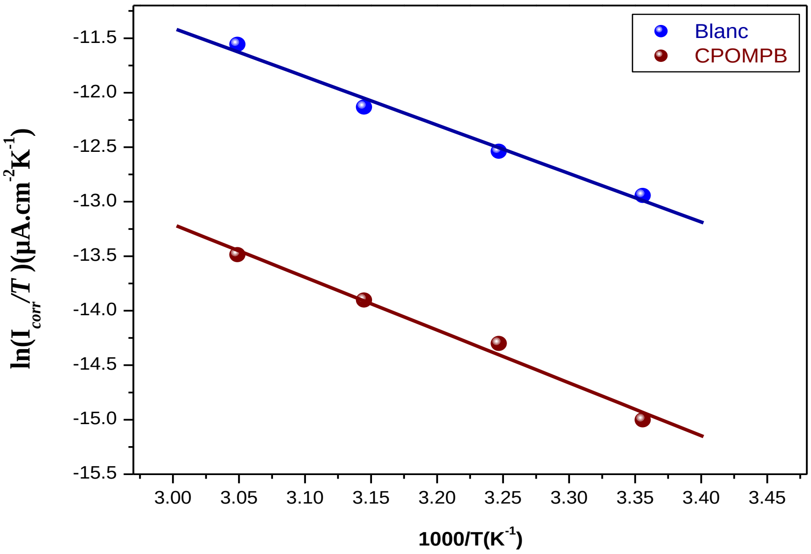

Figure 17: Relation between Ln (I_{corr}/T) and 1000/T at different temperatures.

Table 12: Activation parameters for the corrosion of C-steel in 1.0 M chloridric acid containing different concentrations of inhibitor *CPOMPB.*

Inhibitor	**E_a**	**ΔH^*_a**	**ΔS^*_a**	**E_a - ΔH^*_a**	**ΔG**
	(kJ/mol)	**(kJ/mol)**	**(J/mol)**	**(KJ/mol)**	**(kJ/mol) (T=298K)**
Blank	39.56	36.96	-181.35	2.60	91.01
CPOMPB	42.87	40.27	-186.40	2.60	95.82

The increase in activation energy (***Ea***) of inhibited solutions compared to the blank suggests that inhibitor is physically adsorbed on the corroding metal surface, while either unchanged or lower energy of activation in the presence of inhibitor suggest chemisorption [89]. As reported in Table 12, E_a values increased greatly after the addition of the inhibitor. Hence corrosion inhibition of *CPOMPB* is primarily occurring through physical adsorption. The positive signs of ΔH_a^* reflected the endothermic nature of the C-steel dissolution process.

Another observation is that, for both blank and *CPOMPB* containing solution, the values of ΔH_a^* are lower than the values of the respective activation energies which correspond to a decrease in the total reaction volume due to a gaseous process which is nothing but the hydrogen evolution reaction. Very interestingly the difference of the two values is almost constant with an average value of 2.60 kJ.mol^{-1} which is very close to the average value of the product (RT) in the investigated temperature range. Such behavior is characteristic of a unimolecular gas-phase reaction obeying the following equation [90-97]:

$$E_a - \Delta H_a^* = RT \qquad (12)$$

ΔS_a^* increases negatively with the presence of *CPOMPB* than the uninhibited; this reflects the formation of an ordered stable layer of inhibitor on the steel surface [98].

Temperature is a factor that plays an important role in the corrosion of a given material in a corrosive environment. In the present study, investigation of the influence of temperature on the inhibition efficiency in the absence and presence of 10^{-3} M of *CPOMPB* has been conducted in the temperature range (298- 328 K) and results are reported in table 11.

Although it has been observed according to studies a decreased protective capacity of the inhibitor with increasing temperature [99,100], in our case it was noted that the inhibition efficiency remained stable despite the increase of temperature as depicted in Fig.11, which is very rare to observe among more organic compounds studied.

We note also that this stability of the inhibition efficiency with increasing temperature is of practical interest in processes requiring the protection of the material at high temperature.

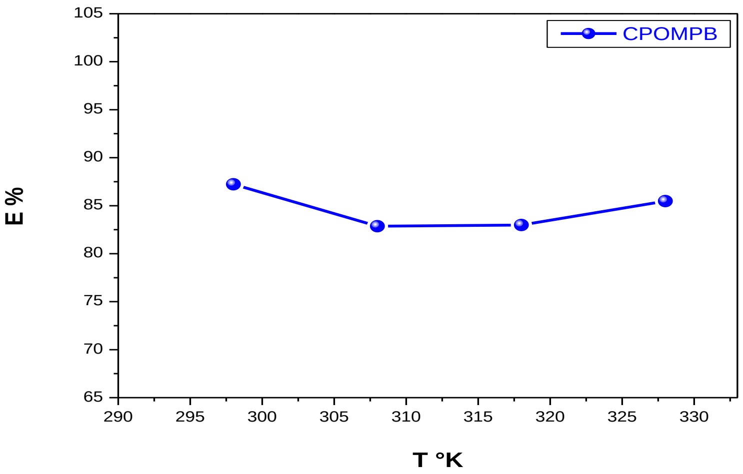

Figure 18: Effect of temperature (298- 328 °K) on the inhibition efficiency (EI%) of carbon steel corrosion in a (10^{-3} M of *CPOMPB* + 1 M HCl) solution.

3.5. *Optical Microscopy Measurements OM*

In order to study the morphology of the carbon steel surfaces in contact with acidic solution, Surface morphology of C38 steel was studied by optical microscopy after 7 days immersion in 1 M HCl before and after addition of the inhibitor. The C38 steel specimens after immersion in 1 M HCl solution at 298K in the absence and presence of optimum concentration of the *CPOMPB*, the specimens were taken out, dried and kept in a dessicator. The optical microscopy images of C38 steel immersed in 1 M HCl in the absence and presence of the optimum concentration of the *CPOMPB* are shown in Fig19 (A, B, C).

The resulting optical microscopy reveal that, the surface was damaged owing to corrosion in absence of the inhibitor (blank), but in presence of the inhibitor, there is a much less damage on the surface. The result was an enhancement of surface coverage and the formation of a good protective film on the steel surface such that there was a decrease in contact between the steel and the aggressive medium. Thus, a good absorptive protection layer can efficiently inhibit the corrosion of steel.

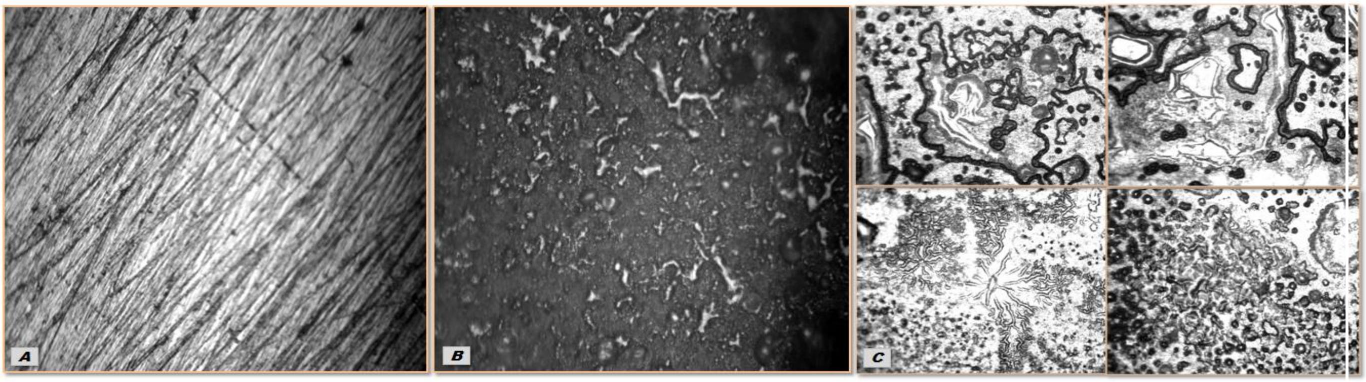

Figure 19: OM (x200) of tinplate (A) before immersion (B) after 7 days of immersion in 1M HCl (C) after 7 days of immersion in 1M HCl + 10^{-3} M of *CPOMPB*.

Conclusion

From the overall experimental results the following conclusions can be deduced:

- *CPOMPB* act as good mild steel corrosion inhibitors in 1M HCl. All electrochemical tests are in good agreement with the maximum percentage of inhibition efficiency obtained at the concentration of 10^{-3} M of *CPOMPB*.
- Potentiodynamic polarization measurements demonstrate that *CPOMPB* act as mixed-type inhibitor.
- The values of apparent activation energy $\boldsymbol{E_a}$ increases with the increase in the inhibitor concentration and suggests that inhibitor is chemically adsorbed on the corroding metal surface and the positive signs of Enthalpy of activation ΔH_a^* reflects the endothermic nature of C-steel dissolution process.
- Thermodynamic investigations confirmed that the adsorption of organic molecule on the mild steel surface obeys The Langmuir adsorption isotherm. The negative values of free energy of adsorption (ΔG_{ads}) indicate that the adsorption process is spontaneous
- The addition of iodide ions to *CPOMPB* enhanced the inhibition efficiency due to synergistic effect and the adsorption of *CPOMPB* alone and in combination with iodide ions obey Langmuir adsorption isotherm.
- From the study of the effect of temperature, it was found that inhibition efficiency (E_I%), very interestingly remained stable despite the increase of temperature and remains around of 85.48 % at 328 °K which is of a practical interest in several industrial processes.

References

1. Trabanelli G., *Corrosion.* 47 (1991) 410–419
2. Manssouri M., El Ouadi Y., Znini M., Costa J., Bouyanzer A., Desjobert J-M., et al. *J Mater Environ Sci.* 6 (2015) 631–646.
3. Anusuya N., Sounthari P., Saranya J., Parameswari K., Chitra S. *J Mater Environ Sci.* 6 (2015) 1606–1623.
4. Hamdi A., Taouti MB., Benbertal D. *J Mater Environ Sci*. 6(2015) 93–100.
5. khandelwal L., Verma CB., Quraishi MA. *J Mater Environ Sci.* 6 (2015) 810–817.
6. Khelifa A., Hamitouche H., Khadraoui A., Hadj Ziane A. *J Mater Environ Sci*. 6 (2015) 1890–1895.
7. Manimegalai S., Manjula P. *J Mater Environ Sci.* 6 (2015) 1629–37.
8. Bouklah M., Hammouti B., Benkaddour M., Benhadda T., *J. Appl. Electrochem.* 35 (2005) 1095-1101.
9. Fiala A., Chibani A., Darchen A., Boulkamh A., Djebbar K., *Appl. Surf. Sci*. 253 (2007) 9347-9356.
10. Fouda A.S., Al-Sarawy A.A., El-Katori E.E., *Desalination.* 201 (2006) 1-13.
11. hamad I. A., Prasad R., Quraishi M.A., *Corros. Sci.* 52 (2010) 1472-1481.
12. Yadav D.K., Maiti B., Quraishi M.A., *Corros. Sci.* 52 (2010) 3586-3598.
13. Edrah S., Hasan S.K., *J. Appl. Sci. Res*. 6 (2010) 1045-1049.
14. Tan Y.J., Bailey S., Kinsella B., *Corros. Sci.* 38 (1996) 1681-1695.
15. Dahmani M., Et-Touhami A., Al-Deyab S.S., Hammouti B., Bouyanzer A., Intern. *J. ELectrochem. Sci*. 5 (2010) 1060-1069.
16. Musa A.Y., Kadhum A.A.H., Mohamad A.B., Takriff M.S., Daud A.R., Kamarudin S.K., *Corros. Sci.* 52 (2010) 526-533.
17. Sherif E.M., Park S.M., *J. Electrochem. Soc*. 152 (2005) B428-B433.
18. Sherif E.M., Park S.M., *Electrochim. Acta*. 51 (2006) 1313-1321.
19. Abd El-Maksoud S.A., Fouda, A.S., *Mater. Chem. Phys*. 93 (2005) 84.
20. Srikanth A.P ., Sunitha T.G ., Raman V., Nanjundan S ., Rajendran N., *Mater. Chem. Phys*. 103 (2007) 241
21. Bouklah M ., Attayibat A., Hammouti B ., Ramdani A ., Radi S., Benkaddour M., *Appl. Surf. Sci*. 240 (2005) 341.
22. Welton T., *Chem. Rev.* 99 (1999) 2071–2083.
23. Davis, J.H., Jr. Task-Specific Ionic Liquids. *Chem. Lett*. 33 (2004) 1072–1077.
24. Cho C.W.; Pham T.P.; Jeon Y.C., Vijayaraghavan K .; Choe W.S.; Yun Y.S., *Chemosphere*, 69 (2007) 1003–1007.
25. Ventura S.P., Goncalves A.M.M., Goncalves F., Coutinho J.A., *Aquat. Toxicol*. 96 (2010) 290–297.

26. Docherty K.M.; Kulpa C.F., *Green Chem*. 7 (2005) 185–189.
27. Endres F., *Chem. Phys. Chem*. 3 (2002) 144–154.
28. Ibrahim M.A.M ., Messali M ., *Prod. Finish*. 2 (2011), 14.
29. Lin Y.F., Sun I.W., *Electrochim. Acta*. 44 (1999) 2771–2777.
30. Liu J ., Jiang G ., Chi Y., Cai Y., Zhou Q ., Hu J., *Anal. Chem*. 21(2003) 5870–5876.
31. Zhang Q.H., Zhang S.G., Deng Y.Q., *Green Chem*. 13 (2011) 2619–2637.
32. Wang J.H., Cheng D.H., Chen X.Y., Du Z., Fang Z.L., *Anal. Chem*. 79 (2007) 620–625.
33. Moniruzzaman M ., Kamiya N ., Goto M., *Org. Biomol. Chem*. 8 (2010) 2887–2899.
34. G Pinto P.C.A., Saraiva M.L.M.F.S., Lima J.L.F.C., *Talanta*. 77 (2008) 479–483.
35. Moniruzzaman M., Nakashima K., Kamiya N., Goto M., *Biochem. Eng. J*. 48 (2010) 295–314.
36. Ibrahim M.A.M., Messali M., Moussa Z., Alzahrani A.Y., Alamry S.N., Hammouti B., *Electrochim. Acta*. 29 (2011) 375–389.
37. Messali M., *J. Mater. Environ. Sci*. 2 (2011) 174–185
38. Zarrouk A., Messali M., Zarrok H., Salghi R., Al-Sheikh Ali A ., Hammouti B., Al-Deyab S.S., Bentiss F., *J.Electrochem. Sci*. 7(2012) 6998–7015.
39. Zarrouk A., Messali M., Aouad M.R., Zarrok H., Salghi R., Hammouti B., Chetouani A., *J. Chem. Pharm. Res.* 4 (2012) 3427–3436.
40. Biswas A., Shogren R.L., Stevenson D.G ., Willett J.L., Bhowmik P.K ., *Carbohydr. Polym.* 66 (2006) 546–550.
41. Da Costa Lopes., João K.G., Morais A.R.C., Bogel-Łukasik E., Bogel-Łukasik R., *Sustain. Chem. Process*. 1 (2013) 3.
42. Wang J. H., Cheng D. H., Chen X. Y., Du Z. and Fang Z. L., *Anal. Chem.* 79 (2007) 620–625.
43. Takahashi S., Koura N., Kohara S., Saboungi M. L. and Curtiss L. A., *Plasmas Ions.* 2 (2009) 91–105.
44. Brennecke J. F. and Magin E. J., *AIChE J.* 47 (2001) 2384–2389
45. De Souza R. F., Padilha J. C., Goncalves R. S., and Rault-Berthelot., *Electrochem. Commun*. 8 (2006) 211–216.
46. Kubisa P., *Prog. Polym. Sci*. 29 (2004) 3–12.
47. Kawano R., Matsui H., Matsuyama C., Sato A., Susan M. A. B. H., Tanabe N.and Watanabe M., *Photochem J. Photobiol. A* 164 (2004) 87–92.
48. Rao C.J., Venkatesan K.A., Nagarajan K ., Srinivasan T.G., Rao P.R.V., *Electrochim. Acta*, 53 (2007) 1911–1919.
49. Pernak J., Sobaszkiewicz K., Mirska I., *Green Chem.* 5 (2003) 52–56.
50. Pernak J., Goc I ., Mirska I., *Green Chem.* 6 (2004) 323–329.
51. Pernak J ., Feder-Kubis J., *Chem. Eur. J.* 11 (2005) 4441–4449.
52. Demberelnyamba D., Lim K.S., Choi S., Park S.Y., Lee H ., Kim C.J., Yoo I.D., *Bioorg. Med. Chem*. 12 (2004)
853–857.
53. Carson L., Chau P.K.W., Earle M.J., Gilea M.A., Gilmore B.F., Gorman S.P., McCann M.T., Seddon K.R., *Green Chem.* 11 (2009) 492–497.
54. Messali M., Moussa Z., Alzahrani A.Y., El-Naggar M.Y ., El Douhaibi A.S., Judeh Z.M.A., Hammouti B., *Chemosphere*. 91 (2013) 1627.
55. Messali M., Almtiri M. N., Bousskri A., Salghi R., Aouad M.R., Alshahateet S.F., Adeeb A-S. Ali. *S. Afr. J. Chem*. 68 (2015**)** 00–00.
56. Ibrahim M.A.M., Messali M., Moussa Z., Alzahrani A.Y., Alamry S.N., Hammouti B., *Portug. Electrochim. Acta*. 29 (2011) 375-389.
57. Messali M., *J. Mater. Environ. Sci.* 2 (2011) 174-185.
58. Zarrouk A., Messali M., Aouad M.R., Assouag M., Zarrok H., Salghi R., Hammouti B., Chetouani A., *J. Chem. Pharm. Res.* 4 (2012) 3427-3436.
59. Messali M. *Acta Pharm.* 65 (**2015**) xx–xx. DOI: 10.1515/acph-2015-0028.
60. Al-Ghamdi A.F., Messali M., Ahmed S.A., *J. Mater. Environ. Sci.* 2 (2011) 215-224.
61. suru T., Haruyama T., Gijutsu S., *B.J. Jpn. Soc. Corros. Eng*. 27 (1978) 573.
62. Aljourani J., Raeissi K., Golozar M.A., *Corros. Sci.* 51 (2009)1836.
63. McCafferty E., Hackerman N . *J Electrochem So.c* (1972) 119-146

64. Gojic M., *Corros. Sci.* 43 (2001) 919–929.
65. Popova A., Raicheva S., Sokolova E., Christov M., *Langmuir.* 12 (1996) 1083–1089.
66. Lopez D.A., Simison S.N., de Sanchez S.R., *Electrochim. Acta* . 48 (2003) 845–854.
67. Popova A., Christov M., Vasilev A., *Corros. Sci*. 49 (2007) 3290–3302.
68. MaCafferty M.and Hackerman N., *Journal of The Electrochemical Society*. 119 (2) (1972) 146–154.
69. Sangeetha M., Rajendran S., Sathiyabama J., Krishnaveni A., Shanthy P., Man-imaran N., Shyamaladevi B., *Port.Electrochim. Acta*. 29 (6) (2011) 429.
70. Rosliza R., Senin H.B., Wan Nik W.B., *Colloids Surf*. 312 (2008) 185.
71. El-Etre A.Y., *Materials Chemistry and Physics*., 108 (2008) 278
72. Umoren S.A. , Obot I. B. , Ebenso E.E., Okafor P. C. , Ogbobe O.and Oguzi E. E., *Anti.corros. Meth. Mater*. 73. (2006) 277-282.
74. Bockris J.O.M., Drazic D., *Electrochem. Acta.*7(1962) 293-313
75. Bentiss F., Gassama F., Barbry D., Gengembre L., Vezin H., Lagrenee M., Traisnel M., *Appl. Surf. Sci*. 252 (2006) 2684.
76. Ajmal M., Mideen A. S., Quraishi M. A., *Corros. Sci*. 36 (1994) 79.
77. Hussin M.H., Kassim M.J., *Mater. Chem. Phys*. 125 (2011) 461.
78. De Souza F.S., Spinelli A., *Corros. Sci.* 51 (2009) 642.
79. El-Awady A.A., Abd-El-Nabey B A., Aziz S G., *J. Electrochem. Soc*. 139 (1992) 2149.
80. O'M J., Bockris, Reddy A.K.N., *Modern Electrochemistry*,vol. 2, (1976),Plenum Publishing Corporation, NewYork.
81. Sanat kumar B.S., Nayak J., Shetty A.N., *J. Coat. Technol. Res.* 4 (2011) 1.
82. Nasshorudin D., *Master dissertation*, Universiti Sains Malaysia. (2010) 20–30.
83. Hussin M.H., Kassim M ., *J.Mater. Chem. Phys*. 125 (2011) 461–468.
84. Benali O., Larabi L., Traisnel M ., Gengenbre L ., Harek Y., *Surf. Sci*. 253 (2007) 6130-6139.
85. Bentiss F., Lebrini M., Lagren´ ee. M., *Corrosion Science*. 4712 (2005) 2915–2931.
86. Li W. H., He Q., Zhang S. T., Pei C. L., and Hou B. R., *Journal of Applied Electrochemistry*. 38 (3) (2008) 289–295.
87. Aramaki K.and Hackerman M., *Journal of The Electro-chemical Society*. 116 (5) (1969) 568–574.
88. Caliskan N. and Bilgic S., *Applied Surface Science*. 153 (2-3) (2000) 128–133.
89. Beck F. T., Kruger U.A., *Electrochim. Acta*. 41 (1996) 1083.
90. Tsuru T., Haruyama S., Gijutsu B. J., *Soc. Corros. Eng*. 27 (1978) 57.
91. Noor E.A., *Intern. J. ELectrochem. Sci.,* 2 (2007) 996-1017.
92. Bouanis F.Z., Bentiss F., Traisnel M., *C. Jama, Electrochim. Acta*, 54 (2009) 2371-2378.
93. Laamari M. R., Benzakour J., Berrekhis F., Abouelfida A., Derja A., Villemin D., *Arab. J. Chem*. 4 (2011) 271-277.
94. Negm N.A., Sabagh A.M.A., Migahed M.A., Bary H.M.A., Din H.M.E., *Corros. Sci*. 52 (2010) 2122-2132.
95. Gomma G.K., Wahdan M.H., *Mater. Chem. Phys*. 39 (1995) 209-213.
96. Antonijevic M.M., Petrovic M.B., *Intern. J. ELectrochem. Sci.* 3 (2008) 1-28.
97. Li X., Mu G., *Appl. Surf. Sci.* 252 (2005) 1254-1265.
98. Yurt A., Balaban A., Kandemir S.U., Bereket G., Erk B., *Mater. Chem. Phys*. 85 (2004) 420.
99. Abd El Rehim S.S., Hassan H.H., Amin M.A., *Mater. Chem. Phys.* 70 (2001) 64-72.
100. Gomma G. K., *Mat. Chem . Phys*. 52 (1998) 200.

(2016) ; http://www.jmaterenvironsci.com